JACS
JOURNAL OF THE AMERICAN CHEMICAL SOCIETY

Communication

pubs.acs.org/JACS

Negatively Charged Lipid Membranes Catalyze Supramolecular Hydrogel Formation

Frank Versluis,[†] Daphne M. van Elsland,[‡] Serhii Mytnyk,[†] Dayinta L. Perrier,[†] Fanny Trausel,[†] Jos M. Poolman,[†] Chandan Maity,[†] Vincent A. A. le Sage,[†] Sander I. van Kasteren,[‡] Jan H. van Esch,[†] and Rienk Eelkema*[,†]

[†]Department of Chemical Engineering, Delft University of Technology, van der Maasweg, 2629 HZ Delft, The Netherlands

[‡]Leiden Institute of Chemistry, Leiden University, P.O. Box 9502, 2300 RA Leiden, The Netherlands

Supporting Information

ABSTRACT: In this contribution we show that biological membranes can catalyze the formation of supramolecular hydrogel networks. Negatively charged lipid membranes can generate a local proton gradient, accelerating the acid-catalyzed formation of hydrazone-based supramolecular gelators near the membrane. Synthetic lipid membranes can be used to tune the physical properties of the resulting multicomponent gels as a function of lipid concentration. Moreover, the catalytic activity of lipid membranes and the formation of gel networks around these supramolecular structures are controlled by the charge and phase behavior of the lipid molecules. Finally, we show that the insights obtained from synthetic membranes can be translated to biological membranes, enabling the formation of gel fibers on living HeLa cells.

In this work we show that negatively charged lipid membranes can act as catalysts for supramolecular hydrogel formation. Reminiscent of natural catalytic processes at the base of many cellular phenomena, (bio)catalysis can be a valuable tool to control the formation and properties of soft self-assembled materials.[1] Furthermore, the groups of Rao, Xu, and others have recently shown that enzymatic activation of synthetic self-assembling molecules in cellular environments leads to promising applications of such molecules as imaging and therapeutic agents.[2] A key challenge in this field is spatial control over the self-assembly. To achieve this, the self-assembling species needs to be formed in the vicinity of the region of interest, after which self-assembly into aggregates effectively immobilizes the formed material. The formation of self-assembling molecules out of nonassembling precursors can be achieved using a variety of stimuli, including pH,[3] light,[4] or chemical reactions.[1c] Here we used negatively charged liposomes to catalyze the formation of a gelator molecule, attempting to control the location of self-assembly to the vicinity of membranes. This would allow the formation of multicomponent hydrogels[5] containing well-defined, enclosed areas that may be used to control the bulk material properties[6a] or to serve as a platform for the controlled release of therapeutic compounds.[6b] Furthermore, it opens up the opportunity of forming fiber networks at cellular interfaces, which can be used to selectively kill malignant cells.[7] Moreover, the long-term potential of fiber formation around cells includes the formation of a synthetic extracellular matrix that might be used to control the communication between cells and their growth and differentiation.

In recent years, we have developed a hydrazone-based supramolecular hydrogelator system[1c,8] that is formed upon reaction between two nonassembling building blocks. Mixing hydrazide **1** and aldehyde **2** building blocks in aqueous media leads to the formation of hydrogelator **3** (Scheme 1), a reaction that proceeds very slowly at pH 7.0. However, using a catalyst (acid or aniline) greatly increases the rate of formation of the gelator. Subsequent self-assembly of **3** into fibers and ultimately a cross-linked fiber network leads to gelation of the surrounding solvent. As negatively charged lipid membranes create a proton gradient in their vicinity through electrostatic interactions, a

Scheme 1. Catalysis by Negatively Charged Membranes[a]

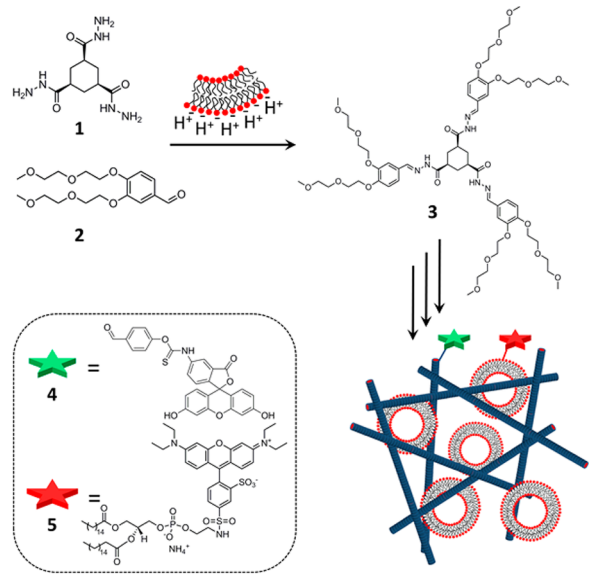

[a]The surface of a negatively charged lipid membrane attracts protons, leading to a local decrease in pH that can catalyze the formation of hydrogelator **3** from nonassembling precursors **1** and **2**. To visualize the gel fibers and lipid membranes, probes **4** and **5**, respectively, are used.

Received: April 14, 2016
Published: June 30, 2016

DOI: 10.1021/jacs.6b03853
J. Am. Chem. Soc. 2016, 138, 8670−8673

lowering of local pH is achieved around the membrane.[8b,9] We were keen to explore whether this slight increase in proton concentration would be capable of catalyzing hydrazone formation to control the formation of synthetic gel fibers (Scheme 1). We first employed well-defined negatively charged liposomes to catalyze gel formation, thereby controlling the physical properties of the gel network. After determining the key parameters of lipid membranes regarding catalytic action and fiber formation, we pursued the formation of gel networks at cellular membranes.

In a typical experiment, phosphate-buffered (100 mM, pH 7.0) stock solutions of **1** and **2** were mixed in a 1:6 ratio to ensure full conversion of hydrazide **1** to hydrogelator **3**. After the immediate addition of a liposomal dispersion in buffer, the mixture was allowed to react at room temperature, leading to formation of **3** and subsequent gelation of the solvent. We first performed minimum gelation concentration (MGC, defined as the lowest concentration of **1** that still forms a gel) experiments to determine the catalytic effect of various liposomes. We used two negatively charged lipids to form liposomes: DPPG and DOPG (see Figure S1 for chemical structures). Liposomes were produced by hydrating a lipid film using sonication, yielding similar size distributions for both batches of liposomes (70−100 nm; Figure S2 and Table S1) with highly negative surface charges (Table S2).

Without addition of catalytic liposomes, gelator **3** has an MGC of 18 mM at pH 7.0. Addition of 5 mM DPPG vesicles decreased the MGC to 2 mM (0.25 wt %) (Figure 1A), which is even slightly lower than the values we previously found for acid- and aniline-catalyzed samples.[1c] In stark contrast, positively charged DPTAP/cholesterol liposomes did not decrease the MGC (Figure 1A). We concluded that the negative charge of membranes is vital for their catalytic activity. To verify this, we studied the formation kinetics of a UV-active hydrazone by mixing 4-hydrazinyl-7-nitrobenz[2,1,3-*d*]oxadiazole[10] and aldehyde **2** (Figure S3A) with and without liposomes. Following the absorbance of the hydrazone product at 480 nm, we observed that the addition of 5 mM DPPG increased the rate of hydrazone formation by a factor of 1.2 compared with either samples lacking liposomes or samples that contained positively charged or zwitterionic liposomes (Figure S3B). These findings indicate that lipid membranes can catalyze hydrazone formation and that the membrane charge is a key parameter. Surprisingly, however, addition of negatively charged DOPG liposomes to precursors **1** and **2** did not induce a lowering of the MGC even at high lipid concentrations. The difference between DPPG and DOPG is the melting temperature of the hydrocarbon chains (T_m = 41 °C for DPPG and −20 °C for DOPG), leading to solid-phase membranes for DPPG and liquid-phase membranes for DOPG at room temperature.[11,12] We therefore hypothesized that the membrane phase behavior is vital for the catalytic turnover of the negatively charged liposomes. To investigate this, we mixed DOPG with cholesterol and prepared liposomes of this binary mixture. Cholesterol is known to increase the rigidity of membranes,[13] and therefore, we expected that these liposomes should lower the MGC significantly. Indeed, we found that mixing in 25 mol % cholesterol with DOPG yielded liposomes that decreased the MGC of our gelator system to around 10 mM (Figure 1A). Moreover, zwitterionic DPPC membranes (ζ = −3.4 mV) showed some catalytic effect, whereas DOPC membranes were completely inactive, confirming the importance of the lipid phase behavior. In conclusion, lipid membranes need to be negatively charged and in the solid phase to efficiently catalyze gel formation. After making these observations, we set out to (1) characterize the DPPG-catalyzed hydrogels, (2) study the mechanism through which gel formation is catalyzed in this multicomponent system, (3) understand why the phase behavior of the lipids is vital for catalytic activity, and (4) develop the first application of this system by growing gel fibers at cellular membranes.

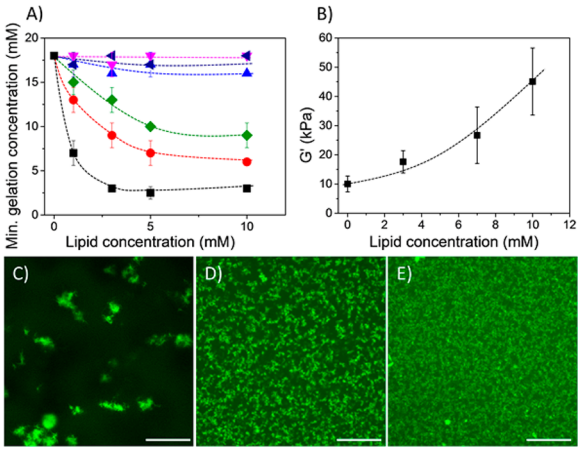

Figure 1. (A) Relationship between MGC, lipid structure, and lipid concentration. Legend: DPPG (black ■); DPPC (red ●); DOPG/Chol (3:1) (green ◆); DOPG (blue ▲); DOPC (dark-blue ◀); DPTAP/Chol (2:1) (magenta ▼). (B) Evaluation of the strength of the gel network as a function of DPPG concentration, measured by rheology. Conditions: 20 mM **1**, 120 mM **2**. (C−E) Influence of DPPG concentration on the morphology of the supramolecular gel networks. The samples contained 3 mM **1**, 18 mM **2**, and 30 μM **4** with (C) 0 mM, (D) 3 mM, and (E) 10 mM DPPG. All experiments were performed in 100 mM phosphate buffer (pH 7.0) at room temperature. All of the lines in (A) and (B) are added to guide the eye, and the scale bars in (C−E) represent 50 μm.

To examine the physical properties of DPPG-catalyzed gel networks, we employed oscillatory rheology (Figure 1B). It is evident that networks with higher storage moduli are obtained when the DPPG concentration is increased (∼45 kPa with 10 mM DPPG vs ∼10 kPa for the uncatalyzed sample, both at 20 mM **1**). These results illustrate the catalytic effect of the negatively charged membranes and show that the physical properties of the gel network can be controlled as a function of lipid concentration. In contrast to previous work,[1c,8c] the gelation time did not decrease with increasing lipid concentration (Figure S4). As we did observe a small but significant catalytic effect of liposomes on hydrazone formation, this observation suggests that the liposomes also act as nucleation points for fiber network formation. Thus, having more liposomes at a higher lipid concentration leads to a more dispersed network and a higher G'.

We characterized the DPPG-catalyzed gel networks further by employing confocal laser scanning microscopy (CLSM). To visualize the gel network, a fluorescein derivative containing an aldehyde functionality (**4**) was mixed with **1**, **2**, and the DPPG liposomes before reaction and gelation. In uncatalyzed samples, slow formation of gelator **3** resulted in large aggregates lacking the ability to form a connected hydrogel network (Figure 1C). In the presence of DPPG liposomes, however, a dense gel network was observed. We also found that increasing the DPPG concentration led to a denser fiber network (Figures 1D,E and S5), enabling us to control the network morphology by varying the phospholipid concentration. Next, we studied the fiber

DOI: 10.1021/jacs.6b03853
J. Am. Chem. Soc. 2016, 138, 8670−8673

morphology using cryo-TEM. The micrographs revealed long, thin gel fibers (typical diameter of 6 nm) and common DPPG liposome morphologies, indicating no clear interactions between the fibers and DPPG liposomes (Figure S6). To corroborate this finding, we performed microcalorimetry to study the phase transition of the liposomes in the absence and presence of gel fibers.[14] No significant change in the phase transition was observed (Figure S7), confirming that the fiber−membrane interactions are negligible.

To investigate the mechanism through which the negatively charged DPPG membranes catalyze gelation, we formed giant vesicles composed of either DPPG/DPPC/Chol (60:20:20) (as pure DPPG does not form stable giant vesicles[15]) or pure DOPG (total lipid concentration 0.2 mM), both with 0.5 μM **5** for fluorescence visualization, using a slow hydration method.[16] We incubated both batches of giant vesicles overnight with precursors **1** and **2** and probe **4**. Surprisingly, we did not observe any gel fibers at the membrane of the DPPG-based vesicles (Figure 2A−C). Upon further inspection of the sample, however,

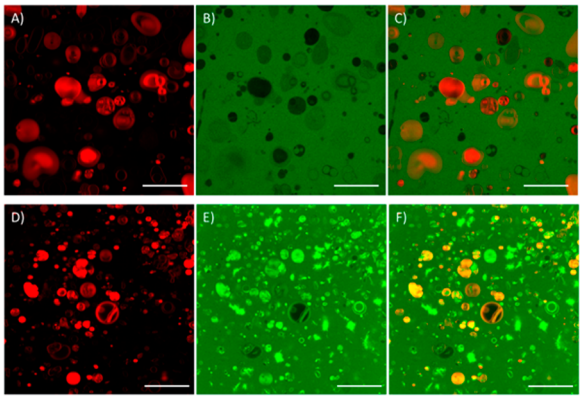

Figure 2. Confocal images of gel fibers with (A−C) DPPG or (D−F) DOPG giant vesicles. **1** and **2** were incubated with the vesicles at 2 and 12 mM, respectively, with 30 μM **4** to visualize the gel fibers (green). Giant vesicle membranes (0.2 mM total lipid concentration) were visualized using 0.5 μM **5** (red). Samples were incubated overnight at room temperature in 10 mM phosphate buffer (pH 7.0). Scale bars: 50 μm.

we found that gel fibers had settled at the bottom of the microscopy well (Figure S8). In contrast, DOPG giant vesicles did show fluorescence of fiber probe **4** at the vesicle surface (Figure 2D−F).

To confirm that this fluorescence intensity was due to the formation of fibers, we performed a control experiment in which only the aldehyde probe (**4**) was added to DOPG liposomes. Here no increased fluorescence intensity at the lipid membranes was observed (Figure S9). Overall, these observations suggest that the affinity of fibers for the interface of lipid membranes is controlled by the phase behavior of the hydrocarbon chains of the lipids. On the basis of the confocal data, it is likely that the gel fibers have an affinity for the liquid-phase DOPG membranes but not for the solid-phase DPPG membranes. To confirm this, we studied the influence of **2** on the structural integrity of small DOPG and DPPG liposomes. As the gel fibers will mainly have this functional group exposed to the solvent (Scheme 1), we expected **2** to interact with the fluid DOPG membranes and not with the solid-phase DPPG membranes. We encapsulated sulforhodamine B at a self-quenching concentration (20 mM) into DOPG and DPPG liposomes and tested the release of the fluorescent probe upon the addition of the aldehyde precursor. Leakage of the probe to the surroundings cancels the self-quenching and is therefore characterized by an increase in fluorescence. As expected, no probe release was observed upon the addition of **2** to DPPG liposomes, whereas the sulforhodamine B concentration in DOPG liposomes quickly equilibrated with its surroundings (Figure S10), although the size (Figure S11) and ζ potential of the DOPG liposomes did not change. These results show that precursor **2** disrupts the structural integrity of the DOPG membranes, and in combination with the confocal data, these observations suggest that the gel fibers interact with the fluid DOPG membranes. As a consequence, the growth of gel fibers specifically around membranes can be controlled as a function of the lipid phase behavior. Moreover, the formation of fiber networks at liquid-phase lipid membranes also supplies us with an explanation for our earlier MGC observations, which showed that liquid-phase DOPG membranes are incapable of inducing the formation of bulk hydrogels. On the basis of the confocal data, it is likely that that the initial formation of gel fibers that bind to the liquid-phase DOPG membranes blocks the surface of these membranes, which therefore are subsequently unavailable for further catalytic action. This process is reminiscent of a typical phenomenon observed with (bio)molecular or heterogeneous catalysts, where the formation of the product inhibits further catalytic action. In stark contrast, the solid-phase DPPG membranes remain free of gel fibers, making their surface continuously available for further rounds of catalysis, explaining their high efficacy in inducing the formation of bulk hydrogels.

Recent research has shown that encapsulating cells in dense gel networks can lead to cell death.[2c,e,h,i] As cell membranes are typically composed of fluid-phase bilayers, we anticipated that it would be possible to grow hydrogel fibers at their surface, which would be detrimental to the viability of the cells. To test this hypothesis, we first used HeLa cells that were fixed using paraformaldehyde and incubated these with precursors **1** and **2** (2 and 12 mM, respectively) overnight at room temperature, together with 30 μM probe **4** to visualize the growth of gel fibers. Confocal microscopy images revealed the formation of brightly fluorescent foci on the HeLa cells, which we attributed to the formation of gel fibers (Figure S12A). The experiment was hampered by unspecific fluorescence staining of the fixed HeLa cells by probe **4**, although these control cells clearly lack the bright foci (Figure S12B). Therefore, to confirm the formation of gel fibers on HeLa cells, we prepared fixed HeLa cells that were treated with **1** and **2** overnight and added the DNA-binding dye DAPI after gelation. Strikingly, very weak nuclear staining of these samples was observed 1 h after DAPI addition (average light intensity 28%), which is in contrast to untreated control samples (100%) (Figure S12C−E). This finding shows the preclusion of this DNA intercalator by the formed hydrogel, thus confirming the formation of gel networks at the HeLa cells.

We next examined whether gel networks could be grown at the surface of living HeLa cells. We incubated **1**, **2**, and **4** (at 0.5 mM, 3 mM, and 30 μM, respectively) at 37 °C with HeLa cells in buffered Dulbecco's modified Eagle's medium (DMEM) (pH 7.4). Confocal microscopy (Figure 3) shows the colocalization of the fluorescence signal of **4** with the HeLa cells. To determine the location of the formed material, we made z-stacks of the cells, which show that the fibers are present throughout the cell (Figure 3C and the supplementary video). To account for its location, we speculate that the material enters the cell through endocytosis. Control experiments in which **4** (Figure S13A−C)

DOI: 10.1021/jacs.6b03853
J. Am. Chem. Soc. 2016, 138, 8670−8673

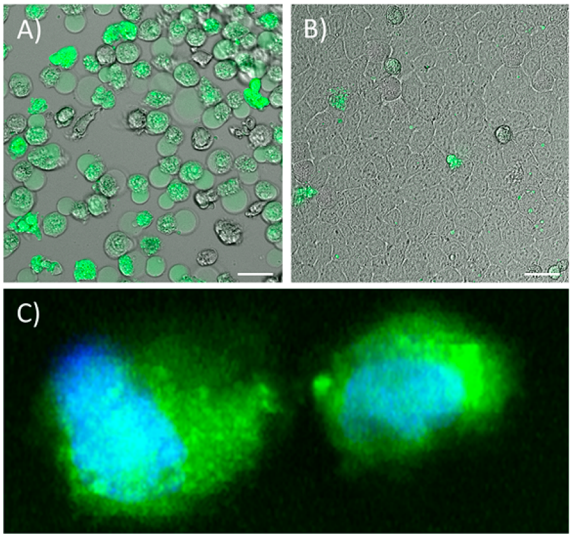

Figure 3. Confocal images showing the formation of gel fibers in HeLa cells. Conditions: (A, C) overnight incubation of 0.5 mM **1**, 3 mM **2**, and 30 μM **4**. (B) Control experiment in which HeLa cells were incubated overnight with 3 mM **2** and 30 μM **4**. (C) 3D reconstruction of a z-stack, revealing the formation of gel fibers throughout the cell. The gel fibers were stained with **4** (green), whereas the nuclei were visualized with Hoechst nuclear dye (blue). All experiments were performed at 37 °C in DMEM. Scale bars: 25 μm.

or a combination of **2** and **4** (Figure 3B) was added to the cells showed only minimal increases in cell-localized fluorescence, indicating that the cell-associated increase in fluorescence of the positive experiment can be attributed to gel formation rather than nonspecific binding of **4** to the cell membrane. After fiber formation, cells were observed to round up and detach from the surface, indicating that the formation of gel fibers is detrimental to the health of the cells. The toxicity of components **1** and **2** was found to be nonexistent at the concentrations used (Table S3), confirming that the structural changes to the cells were caused by fiber formation.

In this paper, we have shown that negatively charged membranes can catalyze the formation of a synthetic fiber network. Using synthetic membranes, we have shown that both the charge and phase behavior of lipid membranes are vital for enabling catalytic activity and the location of fiber formation. Crucially, highly negatively charged liposomes catalyze the formation of the hydrazone gelator most efficiently. Moreover, liquid-phase membranes induce the formation of a gel network at their interface, whereas solid-phase membranes minimize fiber–membrane interactions, keeping this surface available for subsequent catalytic cycles. Finally, we have demonstrated that the results on synthetic membranes can be translated to HeLa cells and that fiber formation around these cells severely limits diffusion of small molecules into the cells.

■ ASSOCIATED CONTENT

Supporting Information

The Supporting Information is available free of charge on the ACS Publications website at DOI: 10.1021/jacs.6b03853.

Experimental details; rheology, microscopy, and spectroscopic data; and cell experiments (PDF)

Visualization of z-stacks of two cells (AVI)

■ AUTHOR INFORMATION

Corresponding Author

*r.eelkema@tudelft.nl

Notes

The authors declare no competing financial interest.

■ ACKNOWLEDGMENTS

We thank The Netherlands Organization for Scientific Research (NWO VIDI Grant to R.E.) and the European Research Council (ERC Starting Grant 639005 to S.I.v.K.) for funding.

■ REFERENCES

(1) (a) Williams, R. J.; Mart, R. J.; Ulijn, R. V. *Biopolymers* **2010**, *94*, 107–117. (b) Yang, Z.; Liang, G.; Xu, B. *Acc. Chem. Res.* **2008**, *41*, 315–326. (c) Boekhoven, J.; Poolman, J. M.; Maity, C.; Li, F.; van der Mee, L.; Minkenberg, C. B.; Mendes, E.; van Esch, J. H.; Eelkema, R. *Nat. Chem.* **2013**, *5*, 433–437. (d) Hardy, M. D.; Yang, J.; Selimkhanov, J.; Cole, C. M.; Tsimring, L. S.; Devaraj, N. K. *Proc. Natl. Acad. Sci. U. S. A.* **2015**, *112*, 8187–8192.

(2) (a) Liang, G.; Ren, H.; Rao, J. *Nat. Chem.* **2010**, *2*, 54–60. (b) Ye, D.; Shuhendler, A. J.; Cui, L.; Tong, L.; Tee, S. S.; Tikhomirov, G.; Felsher, D. W.; Rao, J. *Nat. Chem.* **2014**, *6*, 519–526. (c) Yang, Z.; Liang, G.; Guo, Z.; Guo, Z.; Xu, B. *Angew. Chem., Int. Ed.* **2007**, *46*, 8216–8219. (d) Yang, Z.; Xu, K.; Guo, Z.; Guo, Z.; Xu, B. *Adv. Mater.* **2007**, *19*, 3152–3156. (e) Kuang, Y.; Shi, J.; Li, J.; Yuan, D.; Alberti, K. A.; Xu, Q.; Xu, B. *Angew. Chem., Int. Ed.* **2014**, *53*, 8104–8107. (f) Versluis, F.; van Esch, J. H.; Eelkema, R. *Adv. Mater.* **2016**, *28*, 4576–4592. (g) Yoshii, T.; Mizusawa, K.; Takaoka, Y.; Hamachi, I. *J. Am. Chem. Soc.* **2014**, *136*, 16635–16642. (h) Tanaka, A.; Fukuoka, Y.; Morimoto, Y.; Honjo, T.; Koda, D.; Goto, M.; Maruyama, T. *J. Am. Chem. Soc.* **2015**, *137*, 770–775. (i) Pires, R. A.; Abul-Haija, Y. M.; Costa, D. S.; Novoa-Carballal, R.; Reis, R. L.; Ulijn, R. V.; Pashkuleva, I. *J. Am. Chem. Soc.* **2015**, *137*, 576–579.

(3) Aggeli, A.; Bell, M.; Carrick, L. M.; Fishwick, C. W. G.; Harding, R.; Mawer, P. J.; Radford, S. E.; Strong, A. E.; Boden, N. *J. Am. Chem. Soc.* **2003**, *125*, 9619–9628.

(4) Faramarzi, V.; Niess, F.; Moulin, E.; Maaloum, M.; Dayen, J.-F.; Beaufrand, J.-B.; Zanettini, S.; Doudin, B.; Giuseppone, N. *Nat. Chem.* **2012**, *4*, 485–490.

(5) Wickremasinghe, N. C.; Kumar, V. A.; Hartgerink, J. D. *Biomacromolecules* **2014**, *15*, 3587–3595.

(6) (a) Boekhoven, J.; Koot, M.; Wezendonk, T. A.; Eelkema, R.; van Esch, J. H. *J. Am. Chem. Soc.* **2012**, *134*, 12908–12911. (b) Grijalvo, S.; Mayr, J.; Eritja, R.; Diaz, D. D. *Biomater. Sci.* **2016**, *4*, 555–574.

(7) Zhou, J.; Du, X.; Yamagata, N.; Xu, B. *J. Am. Chem. Soc.* **2016**, *138*, 3813–3823.

(8) (a) Eelkema, R.; van Esch, J. H. *Org. Biomol. Chem.* **2014**, *12*, 6292–6296. (b) Olive, A. G. L.; Abdullah, N. H.; Ziemecka, I.; Mendes, E.; Eelkema, R.; van Esch, J. H. *Angew. Chem., Int. Ed.* **2014**, *53*, 4132–4136. (c) Poolman, J. M.; Boekhoven, J.; Besselink, A.; Olive, A. G. L.; van Esch, J. H.; Eelkema, R. *Nat. Protoc.* **2014**, *9*, 977–988. (d) Maity, C.; Hendriksen, W. E.; van Esch, J. H.; Eelkema, R. *Angew. Chem., Int. Ed.* **2015**, *54*, 998–1001.

(9) Klijn, J. E.; Engberts, J. *J. Am. Chem. Soc.* **2003**, *125*, 1825–1833.

(10) Crisalli, P.; Kool, E. T. *J. Org. Chem.* **2013**, *78*, 1184–1189.

(11) Bensikaddour, H.; Snoussi, K.; Lins, L.; Van Bambeke, F.; Tulkens, P. M.; Brasseur, R.; Goormaghtigh, E.; Mingeot-Leclercq, M.-P. *Biochim. Biophys. Acta, Biomembr.* **2008**, *1778*, 2535–2543.

(12) Findlay, E. J.; Barton, P. G. *Biochemistry* **1978**, *17*, 2400–2405.

(13) Needham, D.; Nunn, R. S. *Biophys. J.* **1990**, *58*, 997–1009.

(14) Boekhoven, J.; Brizard, A. M.; Stuart, M. C. A.; Florusse, L.; Raffy, G.; Del Guerzo, A.; van Esch, J. H. *Chem. Sci.* **2016**, DOI: 10.1039/C6SC01021K.

(15) Himeno, H.; Shimokawa, N.; Komura, S.; Andelman, D.; Hamada, T.; Takagi, M. *Soft Matter* **2014**, *10*, 7959–7967.

(16) Akashi, K.; Miyata, H.; Itoh, H.; Kinosita, K. *Biophys. J.* **1996**, *71*, 3242–3250.

DOI: 10.1021/jacs.6b03853
J. Am. Chem. Soc. 2016, 138, 8670–8673